# Interactions of Atomic Iron Cation with Pyridine and Benzene: A Theoretical Study on an Unresolved Controversy of Bond Energies and Electronic Ground-State Structures

by **Martin Diefenbach**, **Claudia Trage**, and **Helmut Schwarz***

Institut für Chemie der Technischen Universität, Straße des 17. Juni 135, D-10623 Berlin
(fax: +49-30-31421102; e-mail: helmut.schwarz@www.chem.tu-berlin.de)

Dedicated to *Jack D. Dunitz*, a distinguished scientist, inspiring colleague, and dear friend, on the occasion of his 80th birthday

The binding energies, geometries, and electronic structures of cationic iron–benzene and iron–pyridine complexes have been studied by the two hybrid DFT-HF approaches *m*PW1PW91 and B3LYP, as well as the AQCC and MR-AQCC extension. The AQCC results confirm the experimental binding energies derived from threshold-CID experiments reported by *Meyer et al.*, and *Rodgers et al.* as well as the previously reported $C_{2v}$-symmetric quartet ground state of iron–benzene. The iron–pyridine complex is coordinated *via* the N-atom lone-pair and has a sextet ground state. Bond energies determined by the kinetic method apparently yield a dissociation energy corresponding to the first excited quartet iron–pyridine complex. Both DFT methods fail to predict the correct ground state for cationic iron pyridine.

**1. Introduction.** – Since the discovery of ferrocene in 1951 [1–4] and the first efficient synthesis of bis-benzene metal complexes in 1955 [5], organometallic sandwich compounds have been studied extensively by various experimental and theoretical approaches. Sandwich complexes[1]) of heterocyclic aromatic ligands have also been synthesized, *e.g.*, with pyridine as the most basic representative to yield bis($\eta^6$-pyridine)chromium [10]. Cationic systems with a positively charged metal center are quite important in some biological systems [11]; for example, cation–$\pi$ interactions have been observed in the binding site of acetylcholine esterase and alkylamine dehydrogenase [11]. In recent work from *Dunbar* [12][13], and *Bohme* and co-workers [14][15] advanced computational and experimental techniques were applied to probe the complexation of transition-metal cations to arenes and also to more complex $\pi$ systems. Especially for transition-metal systems, cation–$\pi$ interaction beyond simple electrostatic binding is quite prominent. For example, the bond strength of $Na^+$ to benzene ($D_0 = 88.3 \pm 4.3$ kJ mol$^{-1}$) [16] is only less than half that of the $Fe^+$–benzene bond ($D_0 = 207.5 \pm 9.6$ kJ mol$^{-1}$) [17]. Quite helpful for our understanding of the metal–ligand interactions of these systems is knowledge of the thermochemical data, especially bond-dissociation energies (BDEs) of the metal fragment to the aromatic ligands. The gas phase represents a perfect environment in which to study interactions of arenes with isolated ('naked') metal ions, because counter ions, aggregation effects,

[1]) The term 'sandwich complexes' for this class of then novel organometallic compounds was coined by *Wilkinson* [6], and *Dunitz* and *Orgel* [7]. For superb essays on this topic, see [8][9].

solvation, and other complicating bulk effects do not interfere. In this context, mass-spectrometry-based experiments and quantum-chemical calculations complement each other ideally.

In this article, the binding energies of $Fe^+$ to benzene (bz) and pyridine (py) are investigated in some detail. Various experimental BDEs for these two systems have been determined. Using the kinetic method of *Cooks* and co-workers [18][19], *Schröder* and *Schwarz* found $BDE(Fe^+-bz) = 203.3 \pm 8.4\ kJ\,mol^{-1}$ [20]. *Armentrout* and co-workers obtained a threshold-CID value of $207.5 \pm 9.6\ kJ\,mol^{-1}$ [17][21]. In a kinetic modelling study of *Yang* and *Klippenstein* [22], the best estimate for $BDE(Fe^+-bz)$ is a variable-reaction-coordinate transition-state theory (VRC-TST) value of $208.8\ kJ\,mol^{-1}$, though being considered the most uncertain in their systematic study of binding energies of benzene to transition metal cations. *Bauschlicher et al.* performed *ab initio* calculations at the MCPF/DZP level of theory [23]. They assign a $BDE(Fe^+-bz)$ of $213.8\ kJ\,mol^{-1}$ – with an estimated uncertainty of *ca.* $20\ kJ\,mol^{-1}$ – after adjustment of the dissociation asymptote to the experimental $^6D/^4F$ atomic splitting of $Fe^+$ instead of the calculated one. The binding energy of iron–pyridine cation has recently been determined to be $223.7 \pm 8.9\ kJ\,mol^{-1}$ by *Rodgers et al.* in threshold-CID experiments [24]. *Cooks* and co-workers measured $BDE(Fe^+-py) = 205.0 \pm 11.7\ kJ\,mol^{-1}$ by their kinetic method [25]. Another kinetic-method-based binding energy of $BDE(Fe^+-py) = 206.7 \pm 10.0\ kJ\,mol^{-1}$ has been determined in our group [26][27]. In their study on singly- and doubly-charged iron–arene complexes [28] *Kaczorowska* and *Harvey* have also calculated binding energies of $Fe(bz)^+$ and $Fe(py)^+$ by density functional theory and conclude that the bond-energy difference should be of the order of 10 to $30\ kJ\,mol^{-1}$ in favor of $Fe(py)^+$.

The experimental studies on which this work is based used the two mass-spectrometric techniques mentioned above. In the kinetics method, in which branching ratios of competitive dissociations are analyzed, the rates $k_A$ and $k_B$ for either metastable-ion or collision-induced dissociation of a bisligated complex $M(A)(B)^+$ into the monoligated fragments $M(B)^+$ and $M(A)^+$ are related to the difference in binding energy ($\Delta BDE$) of $M^+$ to the ligands A and B, respectively, according to *Eqn. 1*.

$$\Delta BDE = RT_{eff} \ln \frac{k_A}{k_B} \tag{1}$$

Here, $T_{eff}$ is a parameter that describes the effective temperature appropriate for the internal energy of the ions involved upon dissociation. Three requirements that must be met are: *i*) the dissociation proceeds without a barrier, *ii*) the internal energy of the (dissociating) complexes matches the *Boltzmann* distribution, and *iii*) the two ligands are bound to the metal center in a similar fashion. Because the peak ratio of the two fragments can be measured quite accurately, the kinetic method is a rather sensitive tool for the determination of relative BDEs, *i.e.*, in particular small *differences* in binding energies.

In threshold-CID, a molecular-ion beam of the mass-selected monoligated system of interest, *i.e.*, $M(A)^+$ or $M(B)^+$, with a well-defined internal energy is collided with an ideally inert gas at variable energies. The threshold-collision energy for ligand loss then correlates to the binding energy of the ligand to the remaining fragment. This method provides a direct way for the determination of *absolute* binding energies.

Results of recent experiments carried out in our group [26][29] suggest that the relative BDEs for $Fe^+-bz$ and $Fe^+-py$ disagree with the binding energies of $Fe^+-bz$ and $Fe^+-py$ determined in an 'absolute' fashion by *Meyer et al.* [17] and *Rodgers et al.* [24], respectively, as well as with the relative BDEs determined by *Cooks* and co-workers [25]. To elucidate the origins of these discrepancies and to characterize the binding situations in those two molecules, we apply quantum-chemical calculations at various levels of theory.

**2. Computational Details.** – Density-functional calculations were performed with the Gaussian98 [30] program package by means of the widely-used B3LYP [31][32] approach and the *m*PW1PW91 [33] DFT/HF hybrid functional, in conjunction with double-zeta and triple-zeta quality type basis sets. For the monoligated complexes, $Fe(bz)^+$ and $Fe(py)^+$, the all-electron TZV basis set due to *Ahlrichs* and co-workers [34] was used on iron and augmented with two uncontracted *p*-functions with exponents $\alpha = 0.134915$ and 0.041843, and one *f* polarization function ($\alpha = 2.5$) [34]. Carbon, nitrogen, and hydrogen were described by *Pople*'s 6-311 ++ G(d,p) basis sets [35][36]. For the sake of brevity, this basis set is referred to as TZP further below. At this level of theory, geometry optimizations and frequency calculations were performed to identify local minima and transition structures. The bisligated complexes were optimized and characterized as local minima with the unmodified *Ahlrichs*-TZV basis set on iron and 6-31G* basis sets [35] on the nonmetal atoms (DZP basis). Relative energies were subsequently calculated as single points with the larger TZP basis set. To assess the effect of the latter-mentioned *m*PW1PW91/TZP//*m*PW1PW91/DZP approach on geometries and energies, such calculations were performed on the *mono*ligated quartet complexes $Fe(bz)^+$ and $Fe(py)^+$ and compared to the *m*PW1PW91/TZP results. The DZP iron–ligand distances differ by less than 2.5 pm from the TZP geometries, and energies are identical within 0.5 kJ mol$^{-1}$. To account for possible errors in the numerical integration due to low frequency modes, a fine grid of 590 angular *Lebedev* nodes and 99 radial nodes was used in all DFT calculations.

The two different DFT/HF approaches were applied for the following reasons. The B3LYP functional has been shown to provide reasonably accurate geometries and relative energies for many organic as well as several organometallic systems while having modest computational demands [37]. The *m*PW1PW91 functional is specifically parametrized to adequately describe weak as well as noncovalent interactions [33] associated with $\pi$ complexes and transition structures, while, according to a theorem by *Lacks* and *Gordon* [38], retaining accuracy for the description of covalent bonds. As far as transition metals are concerned, recent studies of *Porembski* and *Weisshaar* [39][40] suggest that the latter method is, in fact, more suitable for describing coordinatively unsaturated transition metal compounds than the commonly employed B3LYP approach. Specifically, the proper description of low-spin/high-spin separations in 3d atoms is known to pose problems with B3LYP, where iron constitutes a notoriously problematic case. For example, the previously used B3LYP/6-311 + G* level of theory [41][42] predicts $Fe^+(^4F, 3d^7)$ to be 17 kJ mol$^{-1}$ more stable than $Fe^+(^6D, 3d^6\ 4s^1)$, whereas atomic $Fe^+$ actually has a $^6D$ ground state according to spectroscopy [43][44] with the $^4F$ first excited state 24 kJ mol$^{-1}$ higher in energy. Some improvement is achieved with the larger basis set employed in this work, in that B3LYP/TZP gives the

correct order of ground and excited states, while the computed state splitting of only 0.1 kJ mol$^{-1}$ in favor of $Fe^+$ ($^6$D) is still much too small. Instead, much better agreement is achieved at the *m*PW1PW91/TZP level of theory which predicts the $Fe^+$ ($^4$F) excited state to be 17 kJ mol$^{-1}$ higher in energy than the $Fe^+$ $^6$D ground state.

The use of DFT to compute different spin states of transition-metal compounds has also been discussed by *Reiher* and *Hess* and co-workers [45][46]. They have analyzed the exact exchange part in hybrid density functionals with respect to the prediction of ground state multiplicities. In addition, *Hirao* and co-workers have investigated the performance of various density functionals on transition-metal dimers [47][48].

It is well-known that a single determinant is not necessarily a spin eigenfunction. Furthermore, in transition metal containing molecules near-degeneracy effects can play a role. Thus, only multiconfiguration treatments may provide a realistic picture of such complexes. As a first step, the CASSCF [49] approach accounts for nondynamic correlation. Further, even for a qualitative description of metallic systems, dynamic correlation has to be considered extensively. On the basis of the CAS wavefunction, this can be achieved by multireference variants of many-body perturbation theory (*e.g.*, CASPT2) [50], the multireference averaged coupled-pair functional (MR-ACPF) [51] method, or the multireference averaged quadratic coupled cluster (MR-AQCC) [52] expansion. Classical truncated multireference CI (MRCI) [53] lacks size extensivity and is, therefore, less advisable. For larger sized systems, the MR-AQCC method is probably the most complete treatment of correlation energy presently possible.

However, the latter approach is computationally extremely demanding. Therefore, reasonable compromises between accuracy and computing time are necessary. The reasonably efficient CASPT2 method, though, is not suitable for two reasons. The above-mentioned experimental sextet–quartet splitting of the iron cation cannot be reproduced; for example, a CASPT2 calculation with a 3d 4s active space in conjunction with an atomic natural orbital (ANO) basis set [54] on $Fe^+$ results in a quartet ground state lying 18 kJ mol$^{-1}$ below the sextet state, thereby leading to a wrong ground-state assignment, which may also produce wrong ground-state assignments in the complexes. The AQCC/ANO sextet–quartet state splitting, on the other hand, is 31 kJ mol$^{-1}$ in favor of the $^6$D ground state of $Fe^+$. Second, CASPT2 calculations on the complexes lead to strong intruder-state problems causing the perturbation series to diverge, as reflected by a blow-up of the wavefunction. Therefore, the lowest quartet and sextet states of the $Fe(bz)^+$ and $Fe(py)^+$ complexes were calculated as single points at the RHF-based single-reference AQCC level by means of the *m*PW1PW91/TZV geometries. The lowest states were then computed at MR-AQCC level, and the iron-ligand bond lengths were stepwise re-optimized to an accuracy of 0.1 pm.

For the AQCC and MR-AQCC [52][55][56] calculations, we employed the internally contracted [57] variant available in the MOLPRO [58] suite of programs. Iron was described by the augmented triple-zeta atomic natural orbital (21s 15p 10d 6f 4g)/[8s 7p 5d 3f 2g] basis set of *Pou-Amérigo et al.* [54], carbon and nitrogen by *Dunning*'s correlation-consistent valence triple-zeta (cc-pVTZ) basis sets [59]. For hydrogen, the smaller cc-pVDZ basis set was used [59]. Basis-set effects were examined with a larger quadruple-zeta (VQZ) type basis set, as well as a smaller double-zeta (VDZ) basis set. The VQZ basis consists of the recently published cc-pVQZ (20s 15p 10d 3f 2g 1h)/[6s 8p 6d 3f 2g 1h] basis set of *Ricca* and *Bauschlicher*

[60] on iron and *Dunning*'s cc-pVQZ basis set [59] with up to f primitives on C and N; for H the smaller cc-pVTZ basis set [59] was employed. The VDZ basis comprises *Pou-Amérigo*'s augmented double-zeta ANO (21s 15p 10d 6f)/[6s 5p 4d 2f] basis set for iron and *Dunning*'s cc-pVDZ [59] for the nonmetals. In the RHF-based single-reference AQCC calculations, the 1s 2s 2p 3s 3p(Fe) and the 1s(C) and 1s(N) core electrons were kept frozen. The active space in the CASSCF calculations comprised the 3d 4s(Fe) and $\pi\pi^*$ ligand orbitals, while the remaining twelve occupied valence 2s 2p orbitals of the ligand were always doubly occupied but optimized for each state. In the following internally contracted MR-AQCC computations, no excitations were allowed from those twelve remaining valence and the 15 core orbitals, and all configuration-state functions (CSFs) having a coefficient larger than 0.025 were included as reference functions. Clearly, correlation of all valence orbitals would be highly desirable; however, this exceeds limitations of both the program used and the allocated computational resources. To determine the binding energies, the ground states of isolated $Fe^+$, benzene, and pyridine have been calculated.

**3. Results and Discussion.** – The bond dissociation energies of $Fe(bz)^+$ and $Fe(py)^+$ along with the corresponding $\Delta$BDE values determined by threshold-CID and kinetic methods are given in *Table 1*. Although all values are consistent within their error bars, there are conflicting details. A first notable point is the rather large difference in $\Delta$BDE for the threshold-CID and kinetic methods. According to the threshold-CID measurements, pyridine is over 16 kJ mol$^{-1}$ more strongly bound to $Fe^+$ than benzene, whereas both kinetic approaches yield almost identical binding energies for $Fe(py)^+$ and $Fe(bz)^+$ ($|\Delta BDE| < 2$ kJ mol$^{-1}$). Second, the two values determined with the kinetic method contradict each other in that they yield different signs for $\Delta$BDE. Note that the ratios of benzene *vs.* pyridine losses in each kinetics-method experiment are accurate and reproducible and do not allow for an inversion of sign (for a discussion, see further below).

Table 1. *Bond Dissociation Energies and ΔBDEs*[a]) *for Fe(bz)*$^+$ *and Fe(py)*$^+$ *from Threshold-CID and Kinetic Method Studies.* Values are given in kJ mol$^{-1}$.

| $Fe^+$-bz | Ref. | $Fe^+$-py | Ref. | ΔBDE[a]) | Ref. | Method |
|---|---|---|---|---|---|---|
| $207.5 \pm 9.6$ | [17] | $223.7 \pm 8.9$ | [24] | $-16.2$ | | Threshold-CID |
| | | 209.2[b]) | | $-1.7 \pm 0.9$ | [25] | Kinetics method |
| | | 206.7[b]) | | $0.8 \pm 0.4$ | [26] | Kinetics method |

[a]) The difference in bond dissociation energies is defined as $\Delta BDE = BDE(Fe^+\text{-bz}) - BDE(Fe^+\text{-py})$. [b]) For the sake of consistency, the absolute binding energy is calculated from the experimental $\Delta$BDE value in combination with $BDE(Fe^+\text{-bz})$ from [17]. Note that *Ma et al.* used a different $BDE(Fe^+\text{-bz})$ as anchor point in [25].

We will first discuss our density-functional-theory (DFT) results to assess how the cationic iron complexes are bound and to evaluate the binding energies of $Fe(bz)^+$ and $Fe(py)^+$. In the $Fe(bz)^+$ complex, iron is coordinated to the $\pi$ cloud of the benzene ligand. Pyridine, on the other hand, may bind to $Fe^+$ either as a $\pi$ donor ($Fe^+$ above the ring) or as a $\sigma$ donor ($Fe^+$ in the ring plane), with the lone pair at the N-atom as the coordination site. Next to effects due to charge-induced or ion–dipole interaction, bonding of the metal ion to these ligands is anticipated to be dominated by effects

caused by promotion, hybridization, and orientation of the singly or doubly occupied d orbitals on the metal ion. For $Fe^+$, promotion from the ground state $3d^6\ 4s^1$ electron configuration into the $3d^7$ occupation may lead to a gain in interaction energy, as population of the more compact d orbital reduces the effective size of the ion, thereby allowing it to approach closer to the ligand.

Particularly in the $\pi$-bound complexes, metal d to ligand $\pi^*$ donation may also contribute to binding. It is, thus, most favorable to occupy those d orbitals, which maximize donation into the $\pi^*$ orbitals. Additional electrons must go into orbitals that overlap with $\pi$ orbitals, thereby increasing metal–ligand repulsion. Within $C_{6v}$ symmetry, for example, the metal d orbitals transform as $a_1(d_\sigma)$, $e_1(d_\pi)$, and $e_2(d_\delta)$, the ligand $\pi^*$ orbitals transform according to the $b_1$ and $e_2$ representations. Accordingly, only the $e_2(d_\delta)$ orbitals may, by symmetry restriction, donate into the $\pi^*$ orbitals, because there is no $b_1(d)$ counterpart for the $b_1(\pi^*)$ orbital. The $a_1(d_\sigma)$ overlap is small in face-centered $\pi$ complexes, as the compact orbital points into the 'hole' of the ligand. Thus, the electronic states of the complex are determined by the filling order $e_2(d_\delta)$, $a_1(d_\sigma)$, $e_1(d_\pi)$. In reduced symmetries (*e.g.*, $C_{2v}$), this ordering is assumed to be much less pronounced, because each irreducible representation at the ligand orbitals has a corresponding match in the metal d orbitals.

In the $C_{2v}$-symmetric $\sigma$ complex of $Fe(py)^+$, ordering of the electronic states is determined by metal d to ligand $\sigma$ orbital donation leading to repulsive interaction. The least overlap is given by $d_\delta$ orbitals. $d_\pi$ Orbitals point either towards the ring plane or perpendicularly to the $\pi$ cloud of the ligand, whereas the $d_\sigma$ orbital directly protrudes into the lone pair at the N-atom and will strongly mix with the ligand's molecular orbitals forming the metal–ligand bond, as the lone pair of the N-atom donates into the $d_\sigma$ orbital of iron. Thus, the energetically most favorable orbitals are the $d_\delta$ and $d_\pi$ orbitals, followed by $d_\sigma$.

Table 2. *Relative Energies* [kJ mol$^{-1}$] *for Doublet, Quartet, and Sextet States of Fe(bz)$^+$ and Fe(py)$^+$*

| | Symmetry | State | $E_{rel}$(*m*PW1PW91) | $E_{rel}$(B3LYP) |
|---|---|---|---|---|
| $Fe(bz)^+$ | $C_{2v}$ | $^4A_1$ ($3da_1^4 3da_2^1 3db_1^1 3db_2^1$) | 0.0 | 0.0 |
| | $C_{6v}$ | $^6E_2$ ($3da_1^1 3de_1^2 3de_2^3 4s^1$) | 70.5 | 94.2 |
| | $C_{2v}$ | $^2B_1$ ($3da_1^4 3da_2^2 3db_1^1$) | 128.9 | 119.2 |
| $Fe(\pi\text{-py})^+$ | $C_s$ | $^4A'$ ($3da'^5\ 3da''^2$) | 0.0 | 0.0 |
| | | –[a]) | | |
| | $C_1$ | $^2A$ ($3da^7$) | 94.0 | 88.9 |
| TS[b]) | $C_s$ | $^4A'$ ($3da'^5\ 3da''^2$) | 0.0 | 0.0 |
| | | –[a]) | | |
| | $C_1$ | $^2A$ ($3da^7$) | 112.0 | 102.8 |
| $Fe(\sigma\text{-py})^+$ | $C_{2v}$ | $^4A_1$ ($3da_1^4\ 3da_2^1 3db_1^1 3db_2^1$) | 0.0 | 0.0 |
| | $C_{2v}$ | $^6A_1$ ($3da_1^3\ 3da_2^1\ 3db_1^1\ 3db_2^1\ 4s^1$) | 11.3 | 36.4 |
| | $C_{2v}$ | $^2A_1$ ($3da_1^3\ 3da_2^2\ 3db_1^1\ 3db_2^1$) | 114.8 | 107.2 |

[a]) For the $Fe^+$–pyridine $\pi$ complex, no local minimum could be located at the sextet spin multiplicity PES. The same, consequently, applies to the transition structure. [b]) Transition structure for $\sigma$ to $\pi$ conversion of $Fe(py)^+$.

*DFT Energies and Geometries.* Both, *m*PW1PW91 and B3LYP, predict quartet configurations as the electronic ground states for all complexes, including the transition-state structure between the $\sigma$ and $\pi$ structures of $Fe(py)^+$ (*Table 2*). In $Fe(bz)^+$, the

sextet state is predicted to be by 71 and 94 kJ mol$^{-1}$ higher in energy than the corresponding quartet species at the *m*PW1PW91 and B3LYP levels of theory, respectively. The doublet state is by yet another 58 and 25 kJ mol$^{-1}$, respectively, less stable. Due to the fact that the occupied and virtual $\pi$ orbitals of pyridine are lower-lying than those in benzene, $\pi$ back-bonding from the metal d orbitals appears to play an important role in the structure of these $\pi$ complexes, thus disfavoring high-spin complexes. Accordingly, for the Fe(py)$^+$ $\pi$ complex, no sextet minimum structure could be located, and the absolute energy of the complex rather gradually decreases when approaching the $\sigma$-bound structure; consequently, we assume that there exists no sextet transition structure. The doublet structure of the $\pi$-bound Fe(py)$^+$ complex lies by *ca.* 90 kJ mol$^{-1}$ higher in energy than the corresponding quartet species (*Table 2*). Similarly, the doublet transition structure for the $\sigma$ to $\pi$ conversion of Fe(py)$^+$ is by 112 and 103 kJ mol$^{-1}$, respectively, less favorable than the quartet one. In the Fe(py)$^+$ $\sigma$ complex, the sextet species is – especially at *m*PW1PW91 level (11 kJ mol$^{-1}$; B3LYP: 36 kJ mol$^{-1}$) – quite close to the quartet one, whereas the doublet configurations are by more than 100 kJ mol$^{-1}$ less stable at both DFT levels. In general, *m*PW1PW91 predicts sextet species by *ca.* 15 kJ mol$^{-1}$ lower in energy than B3LYP, which is manifested in the difference in the atomic Fe$^+$ sextet–quartet splitting of 17 kJ mol$^{-1}$ (see above). Similarly, doublet species are *ca.* 5–10 kJ mol$^{-1}$ higher in energy than the B3LYP values. Otherwise, both functionals yield similar ground state wavefunctions and electron configurations.

*Fig. 1* shows the ground state structures of the ligands benzene and pyridine and those of the cationic iron complexes, calculated at *m*PW1PW91/TZP and B3LYP/TZP levels. Both functionals yield similar geometries, B3LYP with a tendency for slightly longer C–C and C–N bonds. In the ligated species, the ligand–iron distances, particularly for the $\pi$ complexes, are predicted to be somewhat shorter at the *m*PW1PW91 level of theory as compared to the B3LYP ones, which is in part probably due to the additional parametrization for noncovalent interactions in the *m*PW1PW91 functional. Unless indicated otherwise, the geometries discussed in the following refer to the *m*PW1PW91 calculations only.

In the quartet ground state of Fe(bz)$^+$, the partial occupation of $3d_\pi$ and $3d_\delta$ orbitals, which are otherwise degenerate in $C_{6v}$ symmetry, results in a modest *Jahn–Teller* distortion to $C_{2v}$ symmetry. In agreement with previous work [22], this produces a boat-shaped ligand with the twofold C-atoms bending toward the metal ion and slightly increased C–C bond lengths. The CCCC dihedral angle amounts to 6°. The $^4A_1$ ground state is derived from a $3d^7$ occupation with doubly occupied orbitals in the $a_1$ irreducible representation, thus donating into the $\pi^*$ orbitals with a doubly occupied $d_\delta$ orbital and, at the same time, keeping repulsion to a minimum with a doubly occupied, compact $d_\sigma$ orbital. The iron–benzene distance is 179 pm (*Fig. 1*). As a result of metal-to-ligand $\pi^*$ donation, the C–C bond lengths of the ligand are *ca.* 1 pm longer than in free benzene. The $^6E_2$ complex exhibits $C_{6v}$ symmetry with an electron occupation that satisfies the above requirements of metal to $\pi^*$ donation, namely, the doubly occupied 3d orbital matches ligand $\pi^*$ orbitals, *i.e.*, it is in the $e_2$ irreducible representation. Due to the larger size of the metal ion in the sextet state derived from a $3d^6\,4s^1$ configuration, the metal–ligand distance of 216 pm is by 37 pm longer than that in the quartet ground-state complex. The C–C bonds in the benzene ligand are only slightly distorted, *i.e.*,

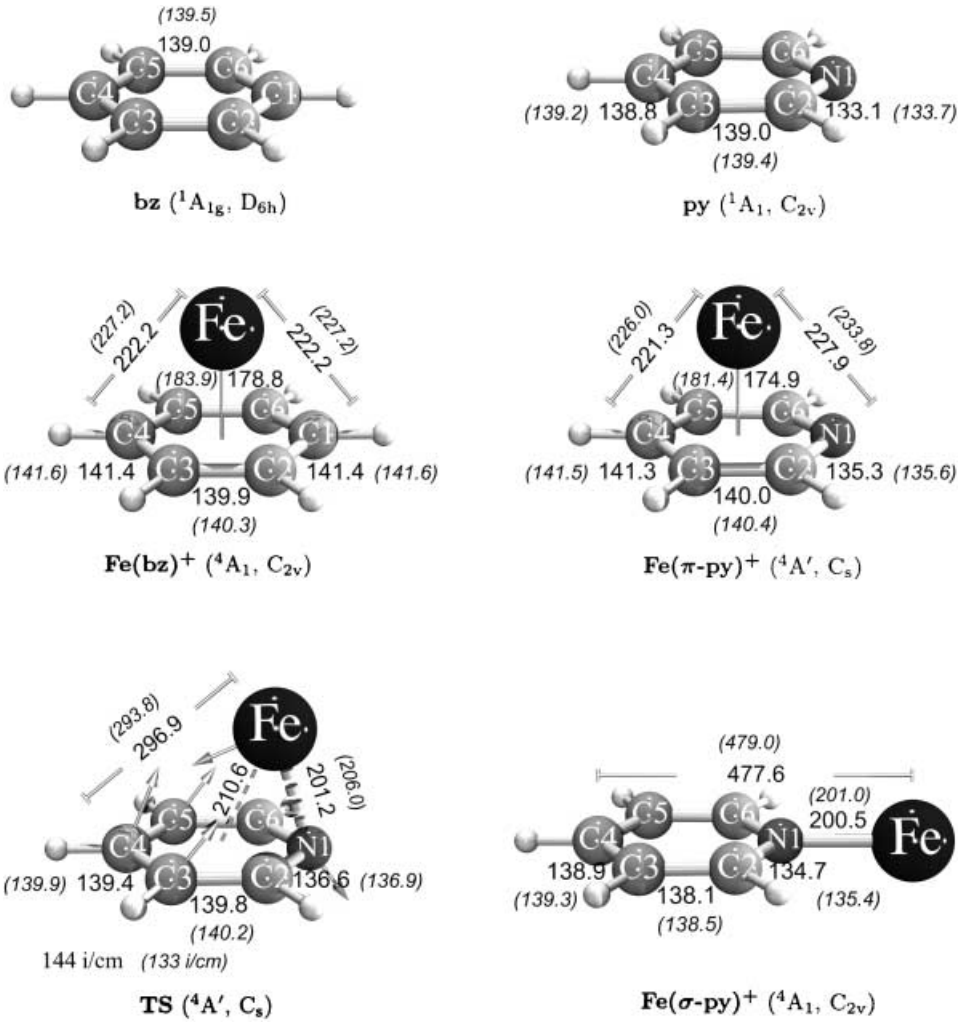


Fig. 1. m*PW1PW91/TZP Geometries of quartet structures of the σ and π complexes of Fe(py)+, the corresponding transition-state structure (TS), and those of pyridine, benzene, and Fe(bz)+*. Bond lengths are given in pm (B3LYP/TZP numbers are in parentheses).

less than 1 pm increased bond length. In the $^2B_1$ state, distortion of the ligand is similar to the quartet case, with a CCCC dihedral of 5°, while the metal–ligand distance of 157 pm is by 22 pm shorter than in the quartet complex (179 pm) due to stronger 3d to $\pi^*$ interaction. Accordingly, the C–C bond lengths are 1 and 3 pm, respectively, longer than in the free ligand.

In the quartet ground state of the $C_s$ symmetric Fe(py)$^+$ $\pi$ complex, the iron cation is located slightly off the center on top of the pyridine ring. The distance of iron to the N-atom is 7 pm longer than that to C(4) (*Fig. 1*), the iron–ligand distance amounts to 175 pm. In analogy to the Fe(bz)$^+$ quartet structure, the pyridine ligand is slightly boat-

shaped where N and C(4) point towards the metal ion, the CCCC dihedral angle is 6° with a CNCC dihedral angle of 7°. The $^4A'$ electronic ground state arises from a configuration with doubly occupied $d_\delta$- and $d_\sigma$-type orbitals of a′ symmetry, giving rise to metal d to ligand $\pi^*$ donation and as little as possible repulsion at the same time, just as in the $Fe(bz)^+$ quartet complex. The ligand's C–N bond length increases by *ca.* 2 pm compared to free pyridine, the C–C distances are 1 and 2 pm longer, respectively. The doublet structure has $C_1$ symmetry due to a slight twist in the pyridine ligand. The iron–pyridine distance is now 167 pm, and the C–C and C–N distances are by 2–3 pm longer than in the free ligand.

Likewise, the transition-state structure between the $\pi$ and $\sigma$ structures of $Fe(py)^+$ exhibits $C_s$ symmetry with a $^4A'$ ground state derived from doubly occupied $d_\delta$- and $d_\sigma$-type orbitals of a′ symmetry. The transition-state structure is very similar to that of the $\pi$-bound complex, and, thus, reactant-like (starting from the $\pi$ complex) according to the *Hammond* postulate. The imaginary mode of 144i $cm^{-1}$ describes a movement of the Fe-atom along the $C_s$ mirror plane toward the center of the ligand and concerted movement of the ligand center towards iron, and *vice versa* (see vector arrows in *Fig. 1*). The doublet transition-state structure has $C_1$ symmetry and is somewhat less similar to the geometry to the $\pi$ complex ($r(Fe–N) = 196$ pm; $r(Fe–C4) = 301$ pm).

The $^4A_1(C_{2v})$ ground state of the $Fe(py)^+$ $\sigma$ complex is derived from a $3d^7$ configuration with doubly occupied $a_1$ orbitals. Thus, metal–ligand repulsion is small due to occupation of a nonbonding $a_1(d_\delta)$ orbital. The pyridine N-atom lone-pair $\sigma$ orbital donates into the other orbital of $a_1$ symmetry, a $d_\sigma$/4s-type hybrid orbital. Note that the $\langle \boldsymbol{S}^2 \rangle$ expectation value of 3.97 in this complex is too high for a quartet spin state and, thus, contains some sextet admixture. The Fe–N bond length is 201 pm, the C–N distance in the pyridine ligand is slightly shorter than in the $\pi$ complex, the C–C bonds are by *ca.* 2 pm shorter; the C(2)–C(3) distance (138 pm) is even shorter than in free pyridine (139 pm). The $^6A_1$ state features a doubly occupied $a_1$ ($d_\delta$) orbital and a singly occupied 4s orbital, which results in a longer Fe–N bond (210 pm), while the ligand bond lengths are almost the same as in the quartet structure. The doublet species has a $C_{2v}$ structure with a 196-pm Fe–N bond and two doubly occupied orbitals of $d_\delta$ and $d_\sigma$ type. The two $d_\pi$-type $b_1$ and $b_2$ orbitals are singly occupied with $\alpha$ spin, the remaining $a_1(d_\delta)$ orbital has a single $\beta$ spin electron. Again, this spin state is associated with sizeable spin contamination ($\langle \boldsymbol{S}^2 \rangle = 1.75$).

In all ground state complexes, the spin density is located at iron. In the $\pi$ complexes and the transition-state structure, the NBO [61] charge distribution leaves a partial charge of $+1.05$ on iron, while, in the $\sigma$ complex of $Fe(py)^+$, some electron transfer from the pyridine ligand to the iron cation results in a partial charge on the metal of $+0.86$ in the quartet state and $+0.90$ in the sextet state, respectively.

*Pyridine* $\sigma$ vs. $\pi$ *Coordination.* Although in most cases pyridine prefers to bind *via* the N-atom lone pair, we have found that $\pi$ coordination is also feasible. An experimental indication for $\sigma$ coordination is the fact that the atomic iron cation accomodates up to four pyridine ligands [62], which would be too many for purely $\pi$ coordinated ligands [15]. *Fig. 2* shows the energy profile for the $\sigma$ to $\pi$ rearrangement of singly-ligated $Fe(py)^+$. Both functionals agree in that the $\sigma$ complex is the ground state structure, the $\pi$ structure lying by 39 (*m*PW1PW91) and 64 kJ $mol^{-1}$ (B3LYP) higher in

energy, respectively. Especially at the B3LYP level, the potential-energy surface is fairly flat in the region of the Fe(py)$^+$ $\pi$ complex with a small barrier (B3LYP: 13 kJ mol$^{-1}$; *m*PW1PW91: 20 kJ mol$^{-1}$) between the $\pi$ complex and the more stable $\sigma$ structure. Both the TS and $\pi$-bound Fe(py)$^+$ are by 17 and 25 kJ mol$^{-1}$, respectively, lower in energy at *m*PW1PW91 than at B3LYP level. Obviously, the $\pi$ complex benefits from the additional parametrization for noncovalent interaction in the *m*PW1PW91 functional.

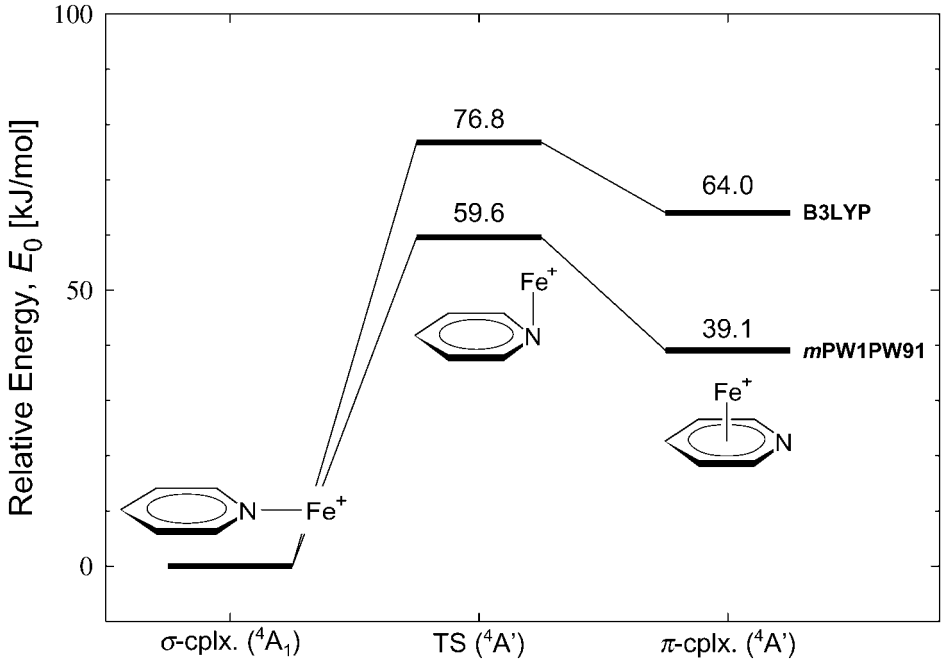


Fig. 2. *Potential-energy surface for $\sigma$ to $\pi$ rearrangement of Fe(py)$^+$, calculated at* m*PW1PW91/TZP and B3LYP/TZP levels of theory.* The energies include zero-point-energy vibrational contributions.

For the evaluation of the kinetic method data, the bisligated complex Fe(bz)(py)$^+$ is also of interest. The two isomers, Fe(bz)$^+$ with a $\sigma$- and with a $\pi$-coordinated pyridine ligand, have been calculated at *m*PW1PW91/TZP//*m*PW1PW91/DZP and B3LYP/TZP//B3LYP/DZP levels. *Table 3* shows that, as with the monoligated Fe(py)$^+$ complex, the $\sigma$-bound bisligated structure is more stable than the sandwich-type $\pi$ complex. Again, the ground state for both complexes is a quartet electron configuration. Next follow doublet configurations, whereas the sextet states are by more than 160 kJ mol$^{-1}$ above the quartet states and thus clearly disfavored energetically at this level of theory.

Table 3. *Relative Energies* [kJ mol$^{-1}$] *for Doublet, Quartet, and Sextet States of Fe(bz)(py)$^+$*

| | Symmetry | State | $E_{rel}$(*m*PW1PW91) | $E_{rel}$(B3LYP) |
|---|---|---|---|---|
| Fe(bz)($\sigma$-py)$^+$ | $C_1$ | $^4$A | 0.0 | 0.0 |
| | $C_1$ | $^2$A | 83.1 | 81.3 |
| | $C_{2v}$ | $^6A_1$ | 168.1 | 181.4 |
| Fe(bz)($\pi$-py)$^+$ | $C_1$ | $^4$A | 87.7 | 89.3 |
| | $C_1$ | $^2$A | 96.4 | 122.0 |
| | $C_1$ | $^6$A | 249.7 | 274.2 |

*DFT Binding Energies.* Besides the absolute binding energies of Fe(bz)$^+$ and Fe(py)$^+$, a pivotal question for the kinetic $\Delta$BDE measurements is which of the two ligands, pyridine or benzene, is more strongly bound to Fe$^+$. *Table 4* shows the bond dissociation energies calculated at *m*PW1PW91/TZP and B3LYP/TZP levels; binding energies refer to the $^6$D(Fe$^+$) ground state asymptote. The basis-set superposition error (BSSE) has been estimated at *m*PW1PW91 level by the *Counterpoise* method [63] and is calculated to be 6–8 kJ mol$^{-1}$. At both levels of theory, $D_0$(Fe$^+$–bz) is identical within 3 kJ mol$^{-1}$ (*m*PW1PW91: 239 kJ mol$^{-1}$; B3LYP: 236 kJ mol$^{-1}$), and it is predicted to be by *ca.* 30 kJ mol$^{-1}$ larger than the experimental value of 208 kJ mol$^{-1}$ measured by *Meyer et al.* [17]. The $\sigma$-bound Fe(py)$^+$ complex, on the other hand, has a binding energy of 229 kJ mol$^{-1}$ according to the *m*PW1PW91 functional and is, thus, smaller than $D_0$(Fe$^+$–bz) but B3LYP predicts $\sigma$-Fe(py)$^+$ to be more strongly bound than Fe(bz)$^+$. The difference in binding energies for $\sigma$-Fe(py)$^+$ at the two levels amounts to almost 27 kJ mol$^{-1}$. Note that the *m*PW1PW91 binding energy of the $\sigma$ complex is in agreement within the estimated experimental uncertainty of $224 \pm 9$ kJ mol$^{-1}$ reported by *Rodgers et al.* [24]. The binding energy of the Fe(py)$^+$ $\pi$ complex, in turn, is almost the same at the *m*PW1PW91 and B3LYP levels, namely 186 kJ mol$^{-1}$. Apparently, not the $\pi$-bound structures but $\sigma$-Fe(py)$^+$ is the molecule that is being described differently by the two functionals, although the distinction is expected to stem from parametrization of noncovalent contributions, including the $\pi$ interaction in the *m*PW1PW91 functional. The differences in binding energies at the two levels of theory amount to $\Delta$BDE(*m*PW1PW91) = 11 kJ mol$^{-1}$ and $\Delta$BDE(B3LYP) = $-19$ kJ mol$^{-1}$. Clearly, this disagreement in calculated $\Delta$BDEs between the *m*PW1PW91 and B3LYP functionals is unsatisfactory: A brief cross-check with other density functionals, however, does not give a conclusive answer. To determine whether the one-parameter exact exchange part in the *m*PW1PW91 functional is responsible for the disagreement, we performed B1LYP calculations, which yield a $\Delta$BDE of $-29$ kJ mol$^{-1}$, *i.e.*, the same sign as the B3LYP one. Using the *un*modified PW91 functional leads to $\Delta$BDE = 24 kJ mol$^{-1}$, which has, in turn, the same sign as the *m*PW1PW91 value. Thus, neither the modification for noncovalent interactions in *m*PW1PW91 nor the difference in exact exchange contribution cause the differences.

*Comparison of the Two Kinetics-Method ΔBDEs. Cooks* and co-workers found that the Fe$^+$–py bond is 1.7 kJ mol$^{-1}$ stronger than that of Fe$^+$–bz compared to a reversed $\Delta$BDE = +0.8 kJ mol$^{-1}$ determined in our group. While, in the experiments of *Schroeter et al.* [26][27], dissociation proceeds *via* metastable ion decay, fragmentation occurs after collision-induced dissociation in the experiments of *Ma et al.* [25]. Additionally, unlike the measurements by *Schroeter et al.*, the results of *Cooks* and co-

Table 4. *DFT BDEs* [kJ mol$^{-1}$] *for Cationic Iron–Benzene and Iron–Pyridine Complexes*

| | | $D_e$[a]) | BSSE | ZPVE | $D_0$[b]) |
|---|---|---|---|---|---|
| $Fe(bz)^+$ | *m*PW1PW91 | 248.3 | – 7.8 | – 1.3 | 239.2 |
| | B3LYP | 244.5 | | – 0.9 | 235.8 |
| $Fe(\sigma\text{-py})^+$ | *m*PW1PW91 | 238.7 | – 5.6 | – 5.0 | 228.6 |
| | B3LYP | 266.0 | | – 5.3 | 255.1 |
| $Fe(\pi\text{-py})^+$ | *m*PW1PW91 | 194.6 | – 7.7 | – 0.9 | 186.0 |
| | B3LYP | 194.0 | | – 0.6 | 185.7 |

[a]) Bond-dissociation energy at zero K. [b]) Bond-dissociation energy at zero K including ZPVE and BSSE correction.

workers could not be obtained *via* direct comparison of BDE($Fe^+$–bz) and BDE($Fe^+$–py) but were determined in two steps *via* ΔBDE(bz/4-$CD_3$-py) and ΔBDE(4-$CD_3$-py/py), because a mass separation of $\Delta m/z = 1$ is difficult to achieve in their quadrupole device, which would be necessary, however, to directly distinguish benzene/$Fe^+$ and pyridine/$Fe^+$. This two-step procedure may be a point of weakness or an additional source of error, because the error increases with increasing mass difference, and the errors of the single measurements are additive. The difference in the two ΔBDEs, however, cannot be explained by merely accounting for this additional source of error.

Although the absolute binding energies reported in *Table 1* refer to 0 K, the relative BDEs from the kinetic method rely on a finite temperature of the dissociating ions ($T_{eff}$), which has been discussed controversially in the literature [64–66], and which may well be another source of error. To investigate possible effects of $T_{eff}$, we computed the temperature dependence of ΔBDE. Both density functionals agree in the thermal behavior such that they give identical, negative slopes as shown in *Fig. 3*. As discussed above, neither *m*PW1PW91 nor B3LYP are capable of reproducing either experimental ΔBDE, and, taken separately, neither graph crosses ΔBDE = 0 in *Fig. 3*. After moving the graph, however, such that it is adjusted to the experimental value at $T_{eff} = 473$ K, sign inversion occurs at *ca.* 1000 K. The trend in temperature dependence of ΔBDE is thus somehow reproduced qualitatively but is by no means quantitatively accurate.

Ab initio *Computations.* As the DFT binding energies do not provide a conclusive answer, obviously, a more-rigorous approach to the determination of binding energies is indicated. To this end, CI-type calculations at averaged quadratic coupled cluster (AQCC) level were employed. Note that the iron–benzene and iron–pyridine complexes cannot necessarily be described with single-reference methods. Contributions from configuration state functions (CSFs) arising from near-degenerate 3d orbitals on iron and from $\pi$ to $\pi^*$ excitation on the ligand are non-negligible. A complete valence-space multireference treatment of these systems, however, is out of question. Therefore, we studied the lowest quartet and sextet states of $Fe(bz)^+$ and $Fe(py)^+$ by the RHF-based single-reference AQCC formalism while including correlation treatment of all valence orbitals. The molecules are calculated as single-points at the *m*PW1PW91/TZV geometries with larger, correlation-consistent basis sets (see *Sect. 2*). Furthermore, multireference AQCC calculations were performed starting from multiconfigurational SCF wavefunctions with 13 electrons in 12 active orbitals (3d

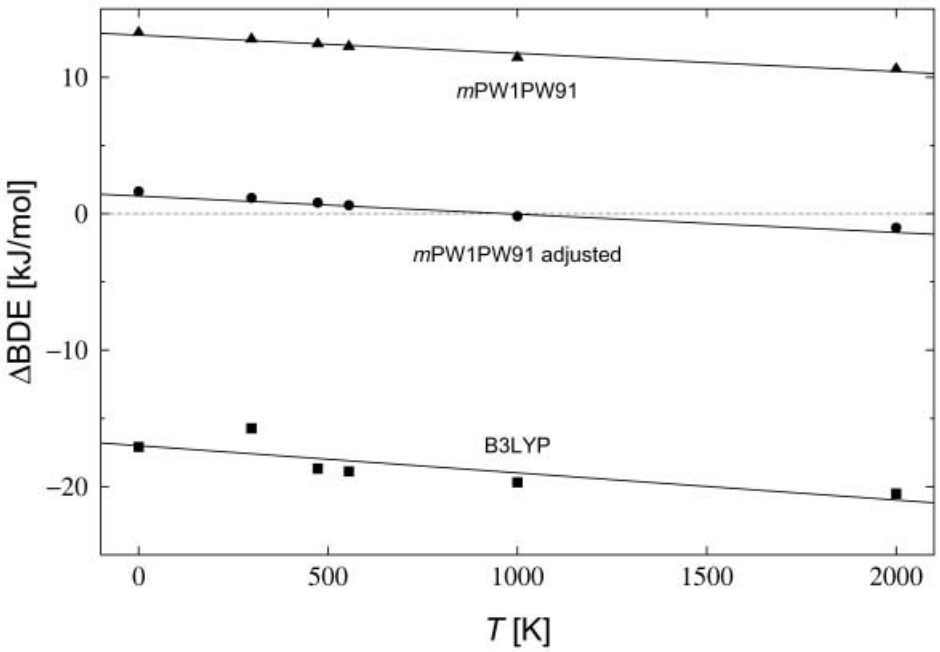


Fig. 3. *Temperature dependence of ΔBDE calculated at DFT level of theory.* Triangles and squares represent *m*PW1PW91 and B3LYP results, respectively, and circles represent empricially adjusted *m*PW1PW91 values (see text).

4s of Fe and $\pi$ $\pi^*$ of the ligand), while the remaining occupied valence orbitals were kept frozen, and only the 12 active and the remaining virtual orbitals were correlated in the subsequent MR-AQCC calculations. At this level of theory, the iron–ligand bond distance was re-optimized.

*AQCC and MR-AQCC Binding Energies. Table 5* contains binding energies for quartet and sextet states of $Fe(bz)^+$ and $Fe(py)^+$. The geometries are taken from the corresponding quartet and sextet *m*PW1PW91/TZP structures. The AQCC results confirm the $^4A_1$ ground state for $Fe(bz)^+$ with a binding energy of 199 kJ mol$^{-1}$, which is within the experimental uncertainty of the threshold-CID value measured by *Meyer et al.* [17]. The nearest sextet state ($^6E_2$) is by 22 kJ mol$^{-1}$ less stable. The iron–pyridine $\sigma$ complex, however, in contrast to the DFT results, possesses a sextet ground state at the AQCC level of theory. The $^6A_2$ state of Fe($\sigma$-py)$^+$ is derived from a doubly occupied $a_2(d_\sigma)$ orbital and is predicted to be by 32 kJ mol$^{-1}$ more stable than the lowest $^4A_2$ electronic state. Note that, again, the calculated binding energy of 230 kJ mol$^{-1}$ is in agreement within the experimental uncertainty of the threshold-CID value (224 ± 9 kJ mol$^{-1}$) reported by *Rodgers et al.* [24]. Similar to the DFT results, the $^4A_2$ state of $Fe(py)^+$ is derived from a doubly occupied $d_\delta$ orbital and a doubly occupied $d_\sigma$ orbital. All quartet states are energetically very close and almost equivalent. The $\pi$-bound $Fe(py)^+$ complex is by 56 kJ mol$^{-1}$ less stable than quartet Fe($\sigma$-py)$^+$ and even 88 kJ mol$^{-1}$ above the sextet ground state of $Fe(py)^+$, thereby confirming that $\pi$

coordination in $Fe(py)^+$ complexes plays, if at all, a minor role. The binding energies of $^4A_1$ $Fe(bz)^+$ and the lowest quartet state $^4A_2$ of $Fe(py)^+$ are almost identical, with $\Delta BDE = 0.4\ kJ\,mol^{-1}$, being close to the $\Delta BDE$ values found by *Schroeter et al.* [26] [29] and *Ma et al.* [25]. This indicates that, in the kinetics-method experiments, starting from bisligated $^4A$ $Fe(bz)(py)^+$ and thus generating, in a spin-allowed dissociation quartet, iron–benzene and iron–pyridine fragments, $\Delta BDE$ is measured as the difference in binding energies of the two quartet species $Fe(bz)^+$ and $Fe(py)^+$, and not as the difference between the two ground state complexes, $^4A_1$ $Fe(bz)^+$ and $^6A_2$ $Fe(py)^+$. Note that despite the erroneous quartet ground state assignment for $Fe(py)^+$ at DFT level, the computed difference between the quartet and sextet states for the bisligated complex $Fe(bz)(py)^+$ is substantially higher ($\Delta E_{m\mathrm{PW1PW91}}(^4A_1/^6A_1\ Fe(py)^+) = 11\ kJ\,mol^{-1}$, $\Delta E_{m\mathrm{PW1PW91}}(^4A/^6A_1\ Fe(bz)(py)^+) = 168\ kJ\,mol^{-1}$). Thus, although the quartet ground state of the $Fe(bz)(py)^+$ could not be confirmed at AQCC and MR-AQCC levels simply for economical reasons, the nearest sextet state lies energetically too high as to be considered relevant for the kinetics-method experiment and for fragmentation to sextet $Fe(py)^+$.

Table 5. *AQCC and MR-AQCC Binding Energies* [$kJ\,mol^{-1}$] *at 0 K of* $Fe(bz)^+$ *and* $Fe(py)^+$. Equilibrium distances $r_e$, *i.e.*, $r(Fe-bz)$ and $r(Fe-N)$, respectively, are given in pm.

| | | | AQCC | | MR-AQCC | | Exper. |
|---|---|---|---|---|---|---|---|
| | | | $T_e$[a]) | $D_e$ | $D_e$ | $r_e$ | $D_e$ |
| $Fe(bz)^+$ | ($C_{2v}$) | $^4A_1$ | 0.0 | 198.9 | 192.5 | 180.6 | $207.5 \pm 9.6$ |
| | | $^4A_2$ | 12.1 | 186.8 | | | |
| | | $^4B_1$ | 61.9 | 137.0 | | | |
| | | $^4B_2$ | 55.8 | 143.1 | | | |
| $Fe(bz)^+$ | ($C_{6v}$) | $^6A_1$ | 34.3 | 164.6 | | | |
| | | $^6E_1$ | 49.6 | 149.2 | | | |
| | | $^6E_2$ | 22.1 | 176.8 | | | |
| $Fe(\sigma\text{-py})^+$ | ($C_{2v}$) | $^4A_1$ | 31.8 | 198.4 | 155.7 | 202.0 | |
| | | $^4A_2$ | 31.6 | 198.5 | 156.9 | | |
| | | $^4B_1$ | 34.8 | 195.4 | 129.9 | | |
| | | $^4B_2$ | 33.2 | 197.0 | 134.1 | | |
| $Fe(\sigma\text{-py})^+$ | ($C_{2v}$) | $^6A_1$ | 0.1 | 230.1 | 194.9 | 213.8 | $223.7 \pm 8.9$ |
| | | $^6A_2$ | 0.0 | 230.2 | 198.6 | | |
| | | $^6B_1$ | 22.1 | 208.1 | 174.0 | | |
| | | $^6B_2$ | 15.9 | 214.3 | 140.9 | | |
| $Fe(\pi\text{-py})^+$ | ($C_s$) | $^4A'$ | 88.0 | 142.2 | | | |
| | | $^4A''$ | 97.6 | 132.5 | | | |

[a]) Term energies relative to the ground-state species.

Both the quartet and sextet states of $Fe(bz)^+$ contain contributions from $\pi$ to $\pi^*$ doubly external configurations with coefficients of *ca.* 0.06, indicating that, for a complete description, those configurations should be taken into account. The external contributions of $\pi$ to $\pi^*$ excitations to the $^6A_2$ state of $Fe(py)^+$ are higher than in $Fe(bz)^+$, and the coefficients amount to 0.07. In the quartet state of $Fe(py)^+$, an additional external configuration due to excitation into the unoccupied 4s orbital appears with a coefficient of 0.16. Accordingly, the 4s orbital of iron is not only

involved in the sextet configurations but also plays a role for the quartet state of $Fe(py)^+$. Thus, for a multireference treatment, the active space in the CASSCF calculations is chosen as 3d 4s(Fe) and $\pi\pi^*$ (ligand). In the subsequent MR-AQCC computations, the remaining 27 occupied orbitals, which also include the 12 occupied 2s 2p valence ligand orbitals next to the 15 core orbitals, are kept frozen.

At MR-AQCC level, the $Fe(bz)^+$ binding energy of 193 kJ mol$^{-1}$ is close to the single-reference AQCC value. The iron–pyridine $\sigma$ complex remains a sextet ground state species but has a binding energy of only 199 kJ mol$^{-1}$, and the quartet Fe($\sigma$-py)$^+$ complex is only bound by 157 kJ mol$^{-1}$. Note that at this level, the BDE of $^4A_2$ $Fe(py)^+$ is by 36 kJ mol$^{-1}$ lower than that of $^4A_1$ $Fe(bz)^+$, while that of $^6A_1$ $Fe(py)^+$ is only by 6 kJ mol$^{-1}$ higher than that of $^4A_1$ $Fe(bz)^+$. The electron configurations for $Fe(bz)^+$ and sextet Fe($\sigma$-py)$^+$ are equivalent in all computational approaches, quartet Fe($\sigma$-py)$^+$, in contrast to the DFT and AQCC results, however, has a fairly high 4s occupation due to strong mixing with the $d_\sigma$ orbital. This phenomenon is already indicated by the large spin contamination of quartet Fe($\sigma$-py)$^+$ in the DFT calculations. The iron–ligand distances are by *ca.* 2–4 pm longer than the *m*PW1PW91/TZP ones. Presumably, upon correlation of the remaining valence orbitals, those bond distances will slightly shorten.

To probe basis-set effects on the binding energies, we performed single-point MR-AQCC calculations on the monoligated complexes $^4A_2$ $Fe(py)^+$, $^6A_2$ $Fe(py)^+$, and $^4A_1$ $Fe(bz)^+$ at the MR-AQCC/triple-zeta geometries with a larger quadruple-zeta basis set (VQZ) as well as a smaller double-zeta basis set (VDZ). For a comparison of 'pure' binding energies without interfering changes in the sextet-quartet splitting of $Fe^+$, *Bauschlicher*'s spin correction [23] was applied. Thus, binding energies of the quartet complexes are calculated with respect to the excited $^4F(Fe^+)$ asymptote and subsequently corrected by the experimental $^6D-{}^4F$ separation (averaged over *J* levels) of 23.94 kJ mol$^{-1}$. The BDE of the quartet iron–pyridine complex decreases gradually from 176 kJ mol$^{-1}$ (VDZ) over 165 kJ mol$^{-1}$ (VTZ) down to 161 kJ mol$^{-1}$ (VQZ) indicating convergence at higher levels and decreasing BDE with increasing basis set; nevertheless, the difference between the triple-zeta and the quadruple-zeta basis sets is quite acceptable. The same difference between VTZ and VQZ binding energies applies to $^6A_2$ $Fe(py)^+$, but with opposite sign, *i.e.*, the BDE of $^6A_2$ $Fe(py)^+$ increases with increasing basis-set size. The different basis sets have virtually no effect on the binding energy of $^4A_1$ $Fe(bz)^+$, which is 200 kJ mol$^{-1}$ in all three cases. Hence, the VTZ basis set is not fully saturated but certainly appropriate for this study.

The MR-AQCC/VQZ calculations also ascertain the sextet ground state of $Fe(py)^+$. The separation between the sextet and quartet state amount to 38 kJ mol$^{-1}$, which compares well with that of the triple-zeta MR-AQCC (42 kJ mol$^{-1}$) and AQCC (32 kJ mol$^{-1}$) values.

One possible reason for the lower bond energies of the MR-AQCC calculations in comparison to the single-reference AQCC ones is the lack of correlation of the remaining twelve occupied ligand 2s 2p valence orbitals describing the ligand ring frame and the C–H bonds. The fact that the $Fe(py)^+$ complexes apparently suffer to a greater extent is in part probably due to the lower-lying $\pi$ and $\pi^*$ orbitals in the pyridine ligand as compared to benzene, which mix more strongly with the ring-frame orbitals. The MR-AQCC extension with 12 active and 27 core orbitals applied in this study

probably is best suited to describe the electronic valence situation in the complexes but also lacks a complete treatment mainly of dynamic correlation. At this point, we, thus, refer to the AQCC binding energies as a basis for discussion.

**4. Conclusions.** – Density functional theory and *ab initio* methods have been used to study cationic iron–benzene and iron–pyridine complexes in terms of electronic structures, geometries, and binding energies. We have found that the $Fe(py)^+$ complex is $\sigma$-bound and has a sextet ground state. Apparently, the DFT methods cannot reproduce the electronic ground state of $Fe(py)^+$, but predict a quartet ground state. Furthermore, the AQCC calculations favor the threshold-CID experiments, *i.e.*, pyridine is clearly more strongly bound to $Fe^+$ than benzene. Even though B3LYP predicts $Fe(py)^+$ to be by 19 $kJ\,mol^{-1}$ stronger bound than $Fe(bz)^+$, this is the right answer for the wrong reason ($Fe(py)^+$ is not quartet). In that respect, *m*PW1PW91 performs better, such that quartet $Fe(py)^+$ is *less* favored over sextet $Fe(py)^+$, that is to say, at B3LYP level, quartet $Fe(py)^+$ is being artificially stabilized. Hence, this is also the case for the two different $\Delta$BDEs calculated at *m*PW1PW91 and B3LYP levels. For a complete description of the electronic structure of the cationic iron–benzene and iron–pyridine complexes, a full-valence multireference treatment would be desirable. Our moderate MR-AQCC calculations show that the 4s(Fe) orbital is also strongly involved in the quartet $Fe(\sigma\text{-}py)^+$ complex, and that correlation of the ligand–ring valence electrons is necessary for the energetic description of the iron–ligand bond.

The kinetics-method experiments start from a bisligated quartet $Fe(bz)(py)^+$ complex that dissociates into the two monoligated quartet species $Fe(bz)^+$ and $Fe(py)^+$. The measured $\Delta$BDE, therefore, corresponds to the difference in binding energies of the two quartet complexes, and not quartet $Fe(bz)^+$ and sextet $Fe(py)^+$. In addition, one of the prerequisites for kinetics-method experiments cannot be met, namely the bisligated complex does not have ligands which are bound to $Fe^+$ in a similar fashion. A possible reason for the deviating signs of the $\Delta$BDE values derived by *Ma et al.* [25] and *Schroeter et al.* [26][27][29] might be the choice of the effective temperature, $T_{eff}$, in the evaluation of the experimental data.

Financial support by the *Deutsche Forschungsgemeinschaft* and the *Fonds der Chemischen Industrie* is appreciated. We are grateful to the *Konrad-Zuse-Zentrum für Informationstechnik Berlin* and the *Zentraleinrichtung Rechenzentrum TU Berlin* for the generous allocation of computer time. The authors thank Dr. *K. Schroeter* and Dr. *D. Schröder* for helpful discussions.

REFERENCES

[1] T. J. Kealy, P. L. Pauson, *Nature* **1951**, *168*, 1039.
[2] S. A. Miller, J. A. Tebboth, J. F. Tremaine, *J. Chem. Soc.* **1952**, 632.
[3] G. Wilkinson, M. Rosenblum, M. C. Whiting, R. B. Woodward, *J. Am. Chem. Soc.* **1952**, *74*, 2125.
[4] E. O. Fischer, W. Pfab, *Z. Naturforsch. B* **1952**, *7*, 377.
[5] E. O. Fischer, W. Hafner, *Z. Naturforsch. B* **1955**, *10*, 665.
[6] G. Wilkinson, *J. Am. Chem. Soc.* **1952**, *74*, 6148.
[7] J. D. Dunitz, L. E. Orgel, *Nature* **1953**, *171*, 121.
[8] J. D. Dunitz, 'Forty Years of Ferrocene', in 'Organic Chemistry: Its Language and Its State of the Art', Ed. M. V. Kisakürek, Verlag Helvetica Chimica Acta, Basel, 1993, pp. 9–23.
[9] P. Lazlo, H. Hoffmann, *Angew. Chem., Int. Ed.* **2000**, *39*, 123.
[10] C. Elschenbroich, J. Koch, J. Kroker, M. Wünsch, W. Massa, G. Baum, G. Stork, *Chem. Ber.* **1988**, *121*, 1983.

[11] J. C. Ma, D. A. Dougherty, *Chem. Rev.* **1997**, *97*, 1303.
[12] R. C. Dunbar, *J. Phys. Chem. A* **2002**, *106*, 7328.
[13] R. C. Dunbar, *J. Phys. Chem. A* **2002**, *106*, 9809.
[14] D. Caraiman, G. K. Koyanagi, L. T. Scott, D. V. Preda, D. K. Bohme, *J. Am. Chem. Soc.* **2001**, *123*, 8573.
[15] D. Caraiman, D. K. Bohme, *Int. J. Mass Spectrom.* **2003**, *223–224*, 411.
[16] P. B. Armentrout, M. T. Rodgers, *J. Phys. Chem. A* **2000**, *104*, 2238.
[17] F. Meyer, F. A. Khan, P. B. Armentrout, *J. Am. Chem. Soc.* **1995**, *117*, 9740.
[18] R. G. Cooks, T. L. Kruger, *J. Am. Chem. Soc.* **1977**, *99*, 1279.
[19] S. A. McLuckey, D. Cameron, R. G. Cooks, *J. Am. Chem. Soc.* **1981**, *103*, 1313.
[20] D. Schröder, H. Schwarz, *J. Organomet. Chem.* **1995**, *504*, 123.
[21] M. T. Rodgers, P. B. Armentrout, *Mass Spectrom. Rev.* **2000**, *19*, 215.
[22] C.-N. Yang, S. J. Klippenstein, *J. Phys. Chem. A* **1999**, *103*, 1094.
[23] C. W. Bauschlicher Jr., H. Partridge, S. R. Langhoff, *J. Phys. Chem.* **1992**, *96*, 3273.
[24] M. T. Rodgers, J. R. Stanley, R. Ammunugama, *J. Am. Chem. Soc.* **2000**, *122*, 10969.
[25] S. Ma, P. Wong, S. S. Yang, R. G. Cooks, *J. Am. Chem. Soc.* **1996**, *118*, 6010.
[26] K. Schroeter, Ph.D. Thesis, Technische Universität Berlin, D83, 2001.
[27] D. Schröder, K. Schroeter, H. Schwarz, *Int. J. Mass Spectrom.* **2001**, *212*, 327.
[28] M. Kaczorowska, J. N. Harvey, *Phys. Chem. Chem. Phys.* **2002**, *4*, 5227.
[29] K. Schroeter, C. Trage, M. Diefenbach, D. Schröder, H. Schwarz, in preparation.
[30] M. J. Frisch, G. W. Trucks, H. B. Schlegel, G. E. Scuseria, M. A. Robb, J. R. Cheeseman, V. G. Zakrzewski, J. J. A. Montgomery, R. E. Stratmann, J. C. Burant, S. Dapprich, J. M. Millam, A. D. Daniels, K. N. Kudin, M. C. Strain, O. Farkas, J. Tomasi, V. Barone, M. Cossi, R. Cammi, B. Mennucci, C. Pomelli, C. Adamo, S. Clifford, J. Ochterski, G. A. Petersson, P. Y. Ayala, Q. Cui, K. Morokuma, D. K. Malick, A. D. Rabuck, K. Raghavachari, J. B. Foresman, J. Cioslowski, J. V. Ortiz, A. G. Baboul, B. B. Stefanov, G. Liu, A. Liashenko, P. Piskorz, I. Komaromi, R. Gomperts, R. L. Martin, D. J. Fox, T. Keith, M. A. Al-Laham, C. Y. Peng, A. Nanayakkara, C. Gonzalez, M. Challacombe, P. M. W. Gill, B. Johnson, W. Chen, M. W. Wong, J. L. Andres, C. Gonzalez, M. Head-Gordon, E. S. Replogle, J. A. Pople, Gaussian98 (Revision A.7), Gaussian, Inc., Pittsburgh PA, 1998.
[31] A. D. Becke, *J. Chem. Phys.* **1993**, *98*, 5648.
[32] P. J. Stephens, F. J. Devlin, C. F. Chabalowski, M. J. Frisch, *J. Phys. Chem.* **1994**, *98*, 11623.
[33] C. Adamo, V. Barone, *J. Chem. Phys.* **1998**, *108*, 664.
[34] A. Schäfer, C. Huber, R. Ahlrichs, *J. Chem. Phys.* **1994**, *100*, 5829, URL ftp://ftp.chemie.uni-karlsruhe.de/pub/basen/fe.
[35] R. Krishnan, J. S. Binkley, R. Seeger, J. Pople, *J. Chem. Phys.* **1980**, *72*, 650.
[36] T. Clark, J. Chandrasekhar, G. W. Spitznagel, P. von Ragué Schleyer, *J. Comput. Chem.* **1983**, *4*, 294.
[37] 'Computational Organometallic Chemistry', Ed. T. R. Cundari, Marcel Dekker, New York, 2001.
[38] D. J. Lacks, R. G. Gordon, *Phys. Rev. A* **1993**, *47*, 4681.
[39] M. Porembski, J. C. Weisshaar, *J. Phys. Chem. A* **2001**, *105*, 4851.
[40] M. Porembski, J. C. Weisshaar, *J. Phys. Chem. A* **2001**, *105*, 6655.
[41] S. Bärsch, D. Schröder, H. Schwarz, *Chem.–Eur. J.* **2000**, *6*, 1789.
[42] S. Bärsch, D. Schröder, H. Schwarz, P. B. Armentrout, *J. Phys. Chem. A* **2001**, 105, 2005.
[43] J. Sugar, C. Corliss, *J. Phys. Chem. Ref. Data* **1985**, *14*, Supplement No. 2, URL http://physics.nist.gov/PhysRefData/.
[44] C. E. Moore, 'Atomic Energy Levels. $^{24}$Cr–$^{41}$Nb', 2nd edn., NSRDS-NBS 35, U.S. Government Printing Office, Washington, DC, 1971, Vol. II.
[45] M. Reiher, O. Salomon, B. A. Hess, *Theor. Chem. Acc.* **2001**, *107*, 48.
[46] O. Salomon, M. Reiher, B. A. Hess, *J. Chem. Phys.* **2002**, *117*, 4729.
[47] S. Yanagisawa, T. Tsuneda, K. Hirao, *J. Chem. Phys.* **2000**, *112*, 545.
[48] S. Yanagisawa, T. Tsuneda, K. Hirao, *J. Comput. Chem.* **2001**, *22*, 1995.
[49] B. O. Roos, P. R. Taylor, P. E. M. Siegbahn, *Chem. Phys.* **1980**, *48*, 157.
[50] K. Andersson, B. O. Roos, P.-Å. Malmqvist, P.-O. Widmark, *Chem. Phys. Lett.* **1994**, *230*, 391.
[51] R. J. Gdanitz, R. Ahlrichs, *Chem. Phys. Lett.* **1988**, *143*, 413.
[52] P. G. Szalay, R. J. Bartlett, *Chem. Phys. Lett.* **1993**, *214*, 481.
[53] P. E. M. Siegbahn, 'The Configuration Interaction Method', in 'Lecture Notes in Quantum Chemistry', Ed. P. O. Roos, Springer, Berlin, 1992, Vol. 58, pp. 255–293.
[54] R. Pou-Amérigo, M. Merchán, I. Nebot-Gil, P.-O. Widmark, B. O. Roos, *Theor. Chim. Acta* **1995**, *92*, 149.

[55] P. J. Knowles, H.-J. Werner, *Chem. Phys. Lett*. **1988**, *145*, 514.
[56] H.-J. Werner, P. J. Knowles, *J. Chem. Phys.* **1988**, *89*, 5803.
[57] H.-J. Werner, P. J. Knowles, *Theor. Chim. Acta* **1990**, *78*, 175.
[58] R. D. Amos, A. Bernhardsson, A. Berning, P. Celani, D. L. Cooper, M. J. O. Deegan, A. J. Dobbyn, F. Eckert, C. Hampel, G. Hetzer, P. J. Knowles, T. Korona, R. Lindh, A. W. Lloyd, S. J. McNicholas, F. R. Manby, W. Meyer, M. E, Mura, A. Nicklass, P. Palmieri, R. Pitzer, G. Rauhut, M. Schütz, U. Schumann, H. Stoll, A. J. Stone, R. Tarroni, T. Thorsteinsson, H.-J. Werner, MOLPRO, a package of *ab initio* programs designed by H.-J. Werner and P. J. Knowles, Version 2002.1, Birmingham, UK, 2002.
[59] T. H. Dunning Jr., *J. Chem. Phys.* **1989**, *90*, 1007.
[60] A. Ricca, C. W. Bauschlicher Jr., *Theor. Chem. Acc.* **2001**, *106*, 314.
[61] J. E. Carpenter, F. Weinhold, *J. Mol. Struct. (THEOCHEM)* **1988**, *169*, 41.
[62] D. K. Bohme, 'Chemistry of $Fe^+$ and Pyridine Measured in the Ion-Chemistry Lab at York University Using ICP/SIFT instrument', personal communication, Feb., 2002.
[63] S. F. Boys, F. Bernardi, *Mol. Phys.* **1970**, *19*, 553.
[64] P. A. Armentrout, *J. Mass Spectrom*. **1999**, *34*, 74.
[65] L. Drahos, K. Vékey, *J. Mass Spectrom*. **1999**, *34*, 79.
[66] R. G. Cooks, J. T. Koskinen, P. D. Thomas, *J. Mass Spectrom*. **1999**, *34*, 85.

*Received January 23, 2003*